

WIKTORIA RATUSZEK *, JANUSZ RYŚ *, MAŁGORZATA KARNAT *

ANNEALING TEXTURES IN COLD-ROLLED DUPLEX TYPE STEEL

TEKSTURY WYŻARZANIA W WALCOWANEJ STALI TYPU DUPLEX

Duplex type austenitic-ferritic steel 00H18N6Mo3 was cold-rolled up to 85% of deformation taking either low or high reductions per pass (variants *A* and *B* respectively) and subsequently annealed at the temperatures 800 and 850°C. X-ray investigations included the phase analysis, measurements of pole figures and calculation of the orientation distribution functions (ODF's) for the case of each phase. Textures of ferrite and austenite after rolling and annealing were analysed within the centre layers of the sheets. The analysis included texture simulation by transformation of experimental ODF's according to Kurdjumov-Sachs (K-S) orientation relationship.

Characteristic feature of deformation and annealing textures in duplex steel under investigation was their fibrous character in both phases, α and γ . The rolling texture of ferrite in duplex steel was strong in comparison to one-phase steels especially for the case of rolling variant *B*. Deformation texture of austenite was relatively weak or nearly random, depending on the rolling variant, even after 85% of reduction. It was concluded that development of ferrite rolling texture may be affected by the phase transformation ($\gamma \rightarrow \alpha$) induced by plastic deformation. During annealing the main changes within the textures of both phases resulted from the transformation of ferrite into austenite ($\alpha \rightarrow \gamma$) as well as the precipitation of the σ phase (FeCr). The crystallographic relationship between the textures of both phases is well described by K-S relation. It seems however that not all of the 24 possible orientations are equally probable and some kind of variant selection takes place during deformation, affecting the resulting annealing texture.

Stal austenityczno-ferrytyczną 00H18N6Mo3 typu duplex walcowano na zimno w zakresie do 85% odkształcenia stosując małe lub duże gnioty częściowe (odpowiednio warianty *A* i *B*) a następnie wyżarzano w temperaturach 800 i 850°C. Badania rentgenowskie obejmowały analizę fazową, pomiary figur biegunowych oraz obliczenia funkcji rozkładu orientacji (FRO) dla każdej z obu składowych faz. Tekstury ferrytu i austenitu po walcowaniu i wyżarzaniu analizowano w warstwie środkowej blach. Analiza obejmowała symulacje tekstury na drodze transformacji eksperymentalnych FRO zgodnie z zależnością Kurdjumowa-Sachsa (K-S).

* WYDZIAŁ METALURGII I INŻYNIERII MATERIAŁOWEJ, AKADEMIA GÓRNICZO-HUTNICZA, 30-059 KRAKÓW, AL. MICKIEWICZA 30

Charakterystyczną cechą tekstur odkształcenia i wyżarzania w walcowanej stali duplex jest ich włóknisty charakter w obu fazach, α i γ . Tekstura walcowania ferrytu w badanej stali duplex była silna w porównaniu ze stalami jednofazowymi zwłaszcza w przypadku wariantu *B*. Natomiast tekstura odkształcenia austenitu była stosunkowo słaba lub niemal bezładna, zależnie od wariantu walcowania, nawet po 85% deformacji. Stwierdzono, że na rozwój tekstury odkształcenia ferrytu może mieć wpływ przemiana fazowa ($\gamma \rightarrow \alpha$) indukowana odkształceniem plastycznym. Podczas wyżarzania zasadnicze zmiany w teksturze obu faz wynikały z przemiany ferrytu w austenit ($\alpha \rightarrow \gamma$) oraz pojawienia się wydzieleni fazy σ (FeCr). Relacje krystalograficzne pomiędzy obiema fazami dobrze opisuje zależność Kurdjumowa-Sachs'a. Wydaje się jednak, że nie wszystkie spośród 24 możliwości są jednakowo prawdopodobne i podczas odkształcenia ma miejsce wybór określonych wariantów, wpływając tym samym na teksturę wyżarzania.

1. Introduction

To a great extent considerable improvement in the properties of duplex type ferritic-austenitic steels is due the character of the structure and results from the favourable combination of the properties of the component phases [1]. Major part of the hitherto performed investigations on austenitic-ferritic steels concerned the effect of chemical composition and thermo-mechanical treatment on the development of two-phase structures. Volume fractions and distribution of the component phases were analysed, grain size and shape as well as the specific surface of the phase interfaces, precipitation of intermetallic phases and other structural factors, which determine the properties of two-phase steels.

However a survey of the investigations concerning duplex type steels points at the insufficient knowledge about the relation between structure and texture after deformation and annealing [2, 3]. In particular formation of deformation textures of the component phases requires further examination, since they determine the textures and structures after annealing and recrystallization and in consequence affect the mechanical properties of two-phase steels [4, 5]. Very important example of such relation, which indicates at texture hardening rather than composite-like reinforcement, is unusually large anisotropy of strength in the case of rolled sheets having the structure consisting of ferrite and austenite bands, forming so-called pancake structure [5, 6].

Another aspect concerning thermo-mechanical behaviour of duplex type steels is the phase instability resulting from chemical composition. In that case not only the ($\alpha \rightarrow \gamma$) phase transformation due to annealing treatment but also deformation induced ($\gamma \rightarrow \alpha$) phase transformation may be the reason of a considerable change of the phase composition and in consequence the change in texture of the component phases [7—10].

The present work concerns the problem of texture development in ferritic-austenitic duplex steel subjected to cold rolling up to 85% of deformation, with low or high reductions per pass, and subsequently annealed at the temperatures 800 and 850°C [11, 12].

The main purpose of the investigation was the analysis of ferrite and austenite annealing textures within the centre layers of the sheets in comparison with the rolling textures of both component phases and the textures of one-phase ferritic and austenitic steels [13—15].

2. Experimental procedure

The material under examination was duplex type austenitic-ferritic steel 00H18N6Mo3. Volume fraction of ferrite was estimated for approximately 43% according to the empirical formula $V_f [\%] = 1.685 (Cr_e - Ni_e - 7.5)^{1.36}$, where Cr_e and Ni_e are chromium and nickel equivalents calculated after equations given for Schaeffler constitution diagram [1]. The above estimation is based only on chemical composition and disregards the effect of thermal treatment on the phase composition of two-phase steels.

Preparation of the material was applied, which included hot working with subsequent annealing and quenching, to equalize the proportions of ferrite (α) and austenite (γ) phases. Material in the form of ingot was homogenized and then subjected to hot forging within the temperature range 900–1000°C. Subsequently the rectangular bars 8 × 20 × 200 mm were annealed at the temperature 1050°C for 3.5 hours and quenched in water. X-ray phase analysis performed after the solution treatment confirmed duplex character of the structure and revealed the volume fraction of ferrite (V_f) of approximately 48% [12].

After the preliminary thermo-mechanical treatment the steel bars were subjected to cold rolling at room temperature up to 85% of deformation ($\epsilon = 1.9$). Reversed rolling without lubricant was applied taking either low reductions per pass or heavy drafts (variants *A* and *B* respectively). Different reductions applied in each roll pass, which depend on the ratio of the arc of contact (L) to the mean thickness (h_m) of the sheet, resulted in different stress and strain distributions on the cross section of the steel being rolled. Different deformation modes were adopted to obtain different contributions of the phase transformation induced by plastic deformation [11].

Following the process of cold-rolling the specimens were annealed at temperatures 800°C for 10 minutes and 850°C for 1 and 10 hours and then quenched in water.

X-ray investigations performed after 85% of rolling reduction and subsequent annealing included qualitative phase analysis and texture measurements using $Co_{K\alpha}$ radiation ($\lambda_{K\alpha} = 1.79$ Å). Additional examination of the state of material was performed by means of the back reflection photographic method.

X-ray phase analysis was carried out by means of diffractometer TuR-M62 equipped with goniometer HZG4. Diffraction patterns were recorded from the centre layers of the sheets for both rolling variants. Texture measurements were performed by the Schulz back-reflection method using the texture attachment TZ6. The incomplete pole figures were recorded of three planes for each of the component phases, namely; {111}, {200}, {220} planes for austenite and {110}, {200}, {211} for ferrite. Measurements of pole figures were conducted within the centre layers of the sheets after 85% reduction, for both rolling variants *A* and *B*, and after annealing at the temperatures 800°C and 850°C.

To obtain a three dimensional texture representation the orientation distribution functions (ODF's) were computed from three incomplete pole figures following the series expansion method described by Bunge [16]. The analysis of the ODF's was

performed in sections of $\varphi_2 = \text{const}$ for the fcc phase (austenite) and for the bcc phase (ferrite) in steps of 5° within the range $0-90^\circ$ (Figs 3 and 4).

Because the rolling and annealing textures of fcc and bcc phases were mostly composed of certain orientation fibres, in addition to the ODF's also the orientation densities along the most important fibres were analysed (Figs 5 and 6).

3. Results and analysis

3.1. Phase analysis

The qualitative phase analysis was performed on the basis of diffraction patterns recorded from the centre layers of the rolled sheets after 85% of reduction and after annealing at the temperatures 800°C for 10 minutes (variant *A* only) and 850°C for 1 and 10 hours, for both variants *A* and *B* (Figs 1a and 1b respectively).

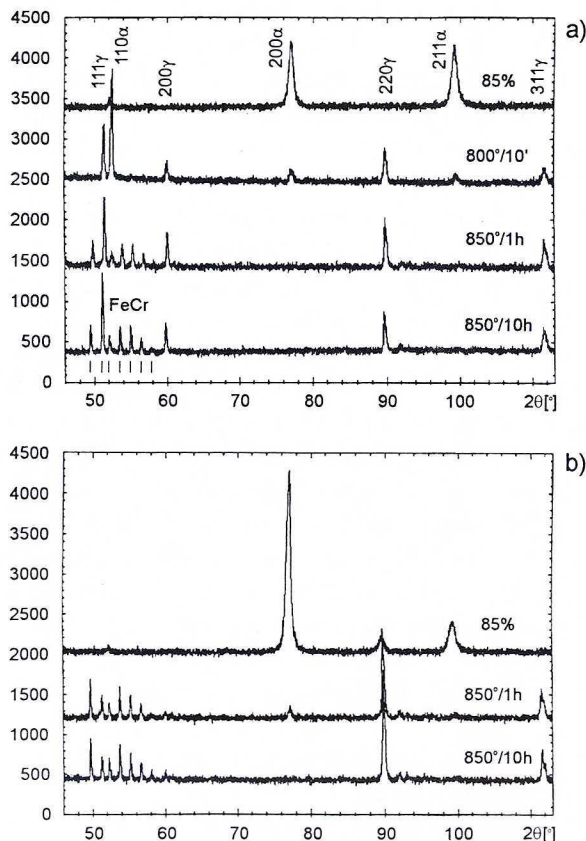


Fig. 1. X-ray diffraction patterns of duplex steel specimens after 85% of deformation and after annealing at 800 and 850°C from the centre layers of the rolled sheets, for rolling variants *A* and *B* (a and b respectively)

Diffraction patterns from specimens cold-rolled up to **85% of deformation** according to the rolling variants *A* and *B* show considerable qualitative differences. In general, for the case of small reductions per pass (variant *A*), the reflections from ferrite phase were mainly revealed with the 200α and 211α two main peaks as well as 111γ reflection from austenite, which has very low intensity. In the case of rolling with heavy drafts (variant *B*) diffraction peaks from both phases are visible, i. e. 200α and 211α from ferrite, with the first one very strong in comparison to rolling variant *A*, and 220γ from austenite.

After **annealing at 850°C** considerable differences in phase composition were detected in comparison to deformed material for rolling variants *A* and *B*. In both cases only reflections 220γ and 311γ from austenite are clearly visible as well as 200γ and 111γ peaks, which have different intensities. Additionally reflections from σ -phase (FeCr) were detected after annealing at 850°C for 1 and 10 hours.

3.2. Texture analysis

Analysis of deformation and annealing textures in ferritic (α) and austenitic (γ) phases was performed after 85% of rolling reduction and after annealing at the temperatures 800°C and 850°C on the basis of the three-dimensional orientation distribution functions (ODF's) calculated from the experimental pole figures.

After **85% of rolling reduction** both component phases developed deformation textures with some typical features of the corresponding rolling textures in one-phase ferritic and austenitic steels, however certain characteristic orientations do not appear or their intensity is very different from those in one-phase steels [13—15].

During **annealing at 800 and 850°C** the main changes within the textures of both phases were connected with the change of phase composition resulting from the transformation of ferrite into austenite ($\alpha \rightarrow \gamma$) as well as the precipitation of the σ phase (FeCr). Similarly to the rolling textures of both phases, some orientation fibres (Figs 5 and 6) may describe the austenite and ferrite annealing textures.

3.2.1. Rolling textures of ferrite

Considering the ferrite texture after 85% of deformation for the case of **variant B**, i. e. high reductions per pass, the rolling texture is described by limited α_1 -fibre, the ϵ and γ orientation fibres as well as orientations of $\{332\} \langle uvw \rangle$ type (Figs 4b and 6b). The limited α_1 -fibre extends from $\{001\} \langle 110 \rangle$ to about $\{111\} \langle 110 \rangle$. Two maxima appeared within that fibre; the first maximum corresponds to the orientation $\{556\} \langle 110 \rangle$ and the second one to $\{001\} \langle 110 \rangle$. Deviation of $\{556\} \langle 110 \rangle$ orientation from the $\{111\} \langle 110 \rangle$ is about 5°. The γ -fibre extends from $\{111\} \langle 110 \rangle$ to $\{111\} \langle 112 \rangle$ having relatively high intensities for both main

components. The ferrite texture includes the ε -fibre running from $\{001\}\langle 100\rangle$ to $\{001\}\langle 110\rangle$ with the strong $\{001\}\langle 100\rangle$ cubic component and $\{001\}\langle 130\rangle$ orientation. Additionally the $\{332\}\langle uvw\rangle$ orientations appeared, namely, $\{332\}\langle 113\rangle$, $\{332\}\langle 110\rangle$ and $\{332\}\langle 023\rangle$.

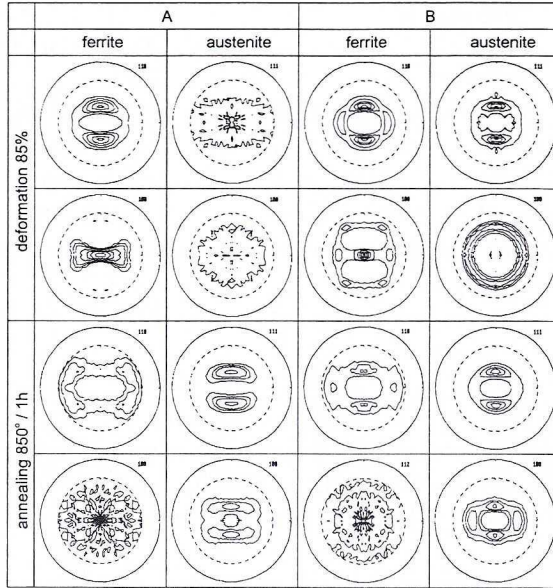


Fig. 2. Experimental pole figures $\{110\}$ and $\{100\}$ of the α -phase and $\{111\}$ and $\{100\}$ of the γ -phase recorded from the centre layers of the sheets, for specimens rolled in variant *A* and *B* after 85% reduction and annealing at 850°C/1 h

In the case of **variant A**, i.e. small reductions per pass (Figs 3b and 6a), a noticeable difference within the ferrite texture is the absence of the γ -fibre, i.e. the $\{111\}\langle 110-112\rangle$ orientations. The limited α_1 -fibre, which extends from $\{001\}\langle 110\rangle$ to $\{223\}\langle 110\rangle$, has the maximum $f(g)$ value for the $\{115\}\langle 110\rangle$ orientation. The ε -fibre is also present after 85% of deformation, however the intensities of the main components are considerably smaller in comparison to variant *B*, especially the intensity of $\{001\}\langle 100\rangle$ orientation. Additional component, which clearly appeared in that case, is the $\{332\}\langle 113\rangle$ orientation.

Characteristic feature of the austenite rolling texture in duplex steel under examination is relatively low intensity or even the absence of some components typical for deformation textures of one-phase austenitic steels.

3.2.2. Deformation textures in austenite

The texture of austenite for the case of **variant B** has the fibre character (Figs 4a and 5b). Within the α -fibre, running from $\{110\}\langle 001\rangle$ to $\{110\}\langle 1\bar{1}0\rangle$, the

strongest is the G o s s orientation $\{110\}\langle 001\rangle$. After 85% reduction another components of that fibre attained relatively high $f(g)$ values, namely; $\{110\}\langle 112\rangle$, $\{110\}\langle 111\rangle$ and $\{110\}\langle 110\rangle$. The second fibre which describes the austenite texture is the η -fibre, which extends from $\{100\}\langle 001\rangle$ to $\{110\}\langle 001\rangle$ and has only one strong component, namely the G o s s orientation (common for both fibres η and α). After 85% reduction, weak orientations of $\{111\}\langle uvw\rangle$ type appeared additionally, namely; $\{111\}\langle 110\rangle$ and $\{111\}\langle 112\rangle$. In general the austenite texture formed in the centre of the sheet is spread (both fibres) and considerably weaker in comparison to the ferrite texture.

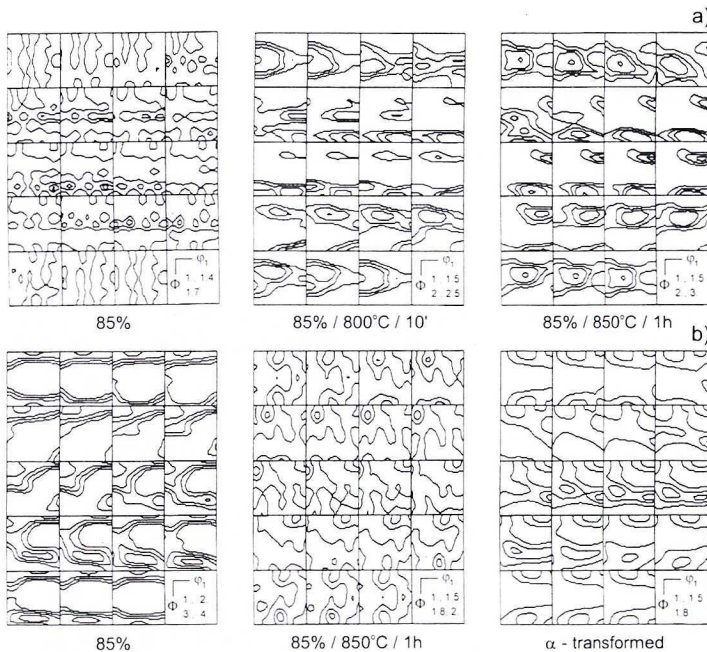


Fig. 3. Orientation distribution functions in sections $\varphi_2 = \text{const}$ for the γ -phase (a) and $\varphi_2 = \text{const}$ for the α -phase (b) after 85% of deformation and annealing (**variant A**, centre layers) and after simulated ($\gamma \rightarrow \alpha$) transformation

Much weaker and nearly random is the texture of austenite when rolling with small reductions per pass, i.e. in **variant A** (Figs 3a and 5a). Noticeable result in that case is the absence of $\{110\}\langle uvw\rangle$ and $\{112\}\langle 111\rangle$ orientations typical for deformation textures of low SFE alloys. Only single and spread components appeared after 85% of deformation, having very low intensities, including $\{111\}\langle 110\rangle$, $\{772\}\langle uvw\rangle$ with the maximum for $\{772\}\langle 027\rangle$ orientation.

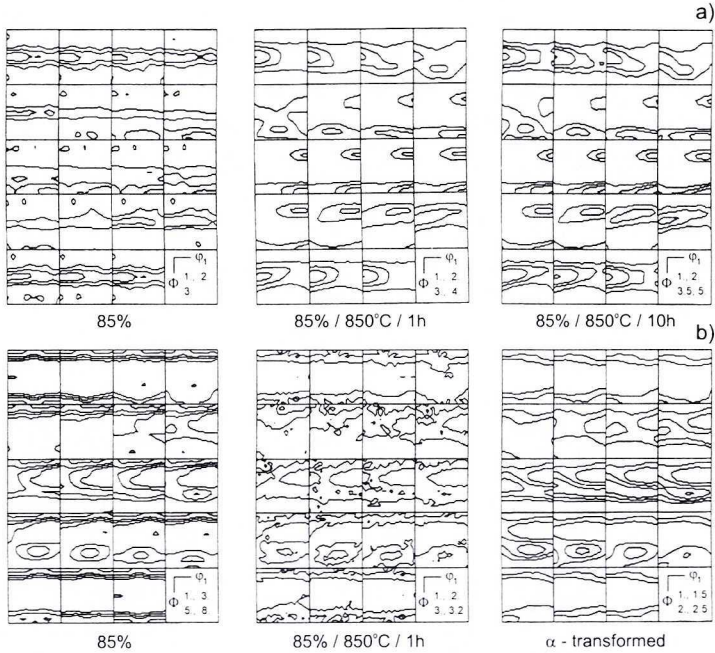


Fig. 4. Orientation distribution functions in sections $\varphi_2 = \text{const}$ for the γ -phase (a) and $\varphi_2 = \text{const}$ for the α -phase (b) after 85% of deformation and annealing (**variant B**, centre layers) and after simulated ($\gamma \rightarrow \alpha$) transformation

3.2.3. Austenite textures after annealing

When analysing the austenite texture for the case of **variant B**, after annealing at 850°C for 1 and 10 hours the α -fibre was found, which extends from $\{110\} \langle 001 \rangle$ to $\{110\} \langle 1\bar{1}0 \rangle$. Similarly to the specimen after 85% reduction the strongest is the G o s s orientation $\{110\} \langle 001 \rangle$ and its intensity increased with the annealing time (Figs 4 and 5). The same situation is for the case of the η -fibre, which extends from $\{100\} \langle 001 \rangle$ to $\{110\} \langle 001 \rangle$ and has only one strong component, namely the G o s s orientation. The only difference in comparison to deformed material is the increase of intensity and spread of the η -fibre after annealing. As to the τ -fibre, which was absent in the austenite rolling texture after 85% reduction (except the $\{110\} \langle 001 \rangle$ orientation) another component appeared after annealing, namely the $\{113\} \langle 332 \rangle$ orientation.

When rolling in **variant A** up to 85% reduction, the texture of austenite was nearly random. However after annealing the limited α -, η -, and τ -fibres or some components from those fibres appeared (Figs 3 and 5). The α -fibre extends from $\{110\} \langle 001 \rangle$ to $\{110\} \langle 1\bar{1}0 \rangle$ for the case of annealing at 800°C for 10 minutes and from $\{110\} \langle 001 \rangle$ to about $\{110\} \langle 554 \rangle$ when annealing at 850°C for 1 hour with the maximum intensity for $\{110\} \langle 112 \rangle$ orientation in both cases. The limited η -fibre, which appeared after annealing for 10 minutes and 1 hour, has the maximum

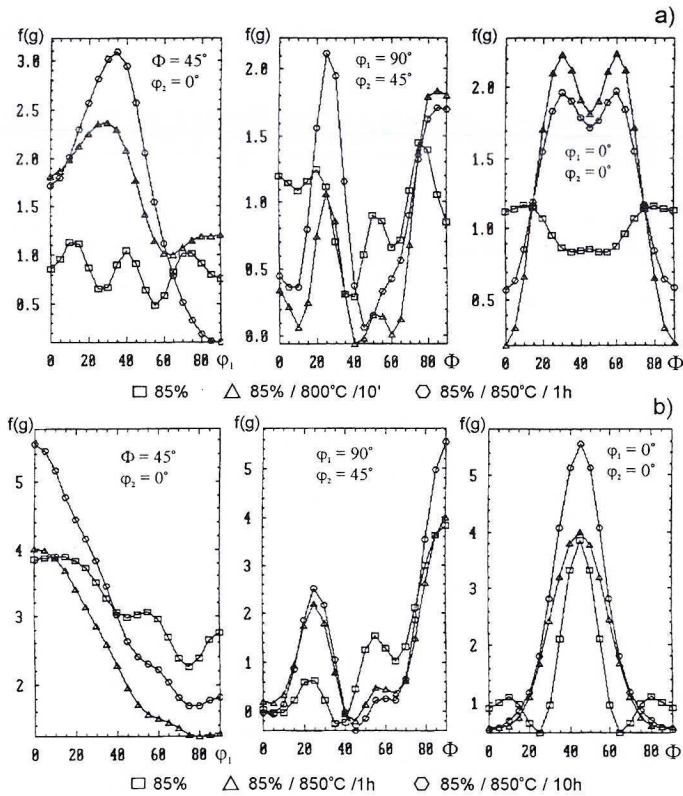


Fig. 5. Values of the orientation distribution function $f(g)$ for the γ -phase along the fibres: $\alpha = \langle 110 \rangle \parallel \text{ND}$, $\tau = \langle 110 \rangle \parallel \text{TD}$ and $\eta = \langle 001 \rangle \parallel \text{RD}$ in specimens after 85% of deformation and annealing (centre layers) for rolling variant *A* (a) and *B* (b)

for $\{320\} \langle 001 \rangle$ and the second relatively strong component $\{110\} \langle 001 \rangle$, i.e. the *G o s s* orientation. Additionally the $\{227\} \langle 774 \rangle$ component from the τ -fibre was detected after annealing at 850°C for 1 hour, which is very close to the $\{113\} \langle 332 \rangle$ orientation.

3.2.4. Annealing textures of ferrite

Comparison of the rolling texture of the α -phase after 85% reduction for the case of **variant B** with the ferrite texture after annealing at 850°C for 10 hours, indicates at considerable decrease of the intensity of all texture components (Figs 4b and 6b). The limited α_1 -fibre extends from $\{001\} \langle 110 \rangle$ to $\{111\} \langle 110 \rangle$ however its intensity is much smaller and the maximum shifted near the orientation $\{113\} \langle 110 \rangle$. Similar results were found for the case of the ε - and γ -fibres, i.e. much weaker intensity and decay of the main component.

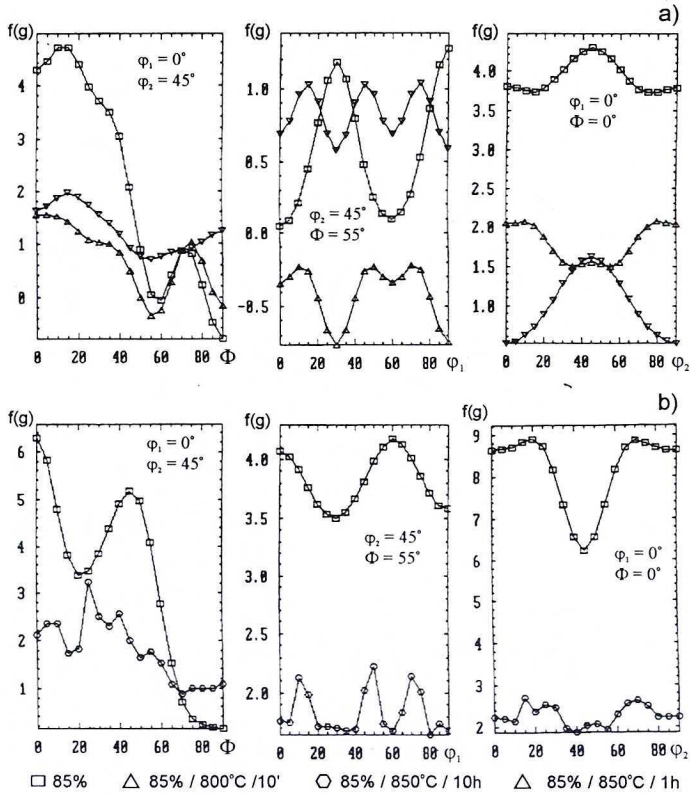


Fig. 6. Values of the orientation distribution function $f(g)$ for the α -phase along the fibres: $\alpha_1 = \langle 110 \rangle \parallel \text{RD}$, $\gamma = \langle 111 \rangle \parallel \text{ND}$ and $\varepsilon = \langle 001 \rangle \parallel \text{ND}$ in specimens after 85% of deformation and annealing (centre layers) for rolling variant *A* (a) and *B* (b)

In the case of the rolling **variant A** (Figs 3b and 6b) the absence of the γ -fibre, i.e. the $\{111\} \langle 110-112 \rangle$ orientations, within the ferrite texture after annealing is still observed. The intensity of the limited α_1 -fibre, which extends from $\{001\} \langle 110 \rangle$ to about $\{112\} \langle 110 \rangle$, with the maximum for $\{115\} \langle 110 \rangle$ orientation, considerably decreased after annealing at 850°C for 1 hour. The weak ε -fibre is present after annealing at 800°C for 10 minutes, however the intensities of the main components are considerably smaller in comparison to deformed material. Further annealing resulted in decay of the $\{001\} \langle 100 \rangle$ component and weakening of the $\{001\} \langle 110 \rangle$ orientation.

4. Discussion

Copper type $\{112\} \langle 111 \rangle$ component and orientations laying within its spread, i.e. $\{113\} \langle 332 \rangle$ and $\{227\} \langle 774 \rangle$, were not found in the texture of austenite after 85% of deformation (the centre layers of the rolled sheets). On the other hand, the

$\{113\}\langle 332\rangle$ orientation (or the $\{227\}\langle 774\rangle$ component) clearly appeared within the austenite annealing textures in the case of both variants *A* and *B*. Deviation of the $\{227\}\langle 774\rangle$ orientation from the $\{113\}\langle 332\rangle$ is about 3° and both orientations belong to the τ -fibre.

The $\{112\}\langle 110\rangle$ and $\{113\}\langle 110\rangle$ orientations, found within the rolling and annealing textures of ferrite, are in *K-S* relation with the $\{112\}\langle 111\rangle$ and $\{113\}\langle 332\rangle$ orientations, which were not detected in austenite rolling texture after 85% reduction. It is assumed therefore, that austenite grains having such orientations undergo the ($\gamma \rightarrow \alpha$) phase transformation during deformation and hence the appearance of the $\{112\}\langle 110\rangle$ and $\{113\}\langle 110\rangle$ orientations within the ferrite deformation texture. Additionally if the same orientations, as detected after annealing, arise from the inverse ($\alpha \rightarrow \gamma$) transformation, this result may indicate a possibility of the temporary appearance of the $\{112\}\langle 111\rangle$ and $\{113\}\langle 332\rangle$ orientations in successive grains during development of austenite rolling texture. According to J o n a s et al. [7–9], the $\{113\}\langle 110\rangle$ and $\{112\}\langle 110\rangle$ components of the ferrite texture result from the transformation of copper type texture $\{112\}\langle 111\rangle$ during quenching but only in the case when the ferrite and austenite bands form so-called pancake structure. This result is attributed to be the effect of grain aspect ratio on variant selection during the ($\gamma \rightarrow \alpha$) phase transformation [7].

The α -fibre, $\{110\}\parallel\text{ND}$, was nearly absent in austenite texture after 85% of deformation for the case of rolling variant *A* (Fig. 5a) and quite well pronounced when rolling in variant *B* (Fig. 5b). Within the annealing textures of austenite some orientations of the α -fibre are observed, however the main components are different in both variants. For the case of variant *A*, the highest intensity has the $\{110\}\langle 112\rangle$ orientation (Fig. 5a) and in variant *B*, the $\{110\}\langle 001\rangle$ component (Fig. 5b). During annealing the inverse ($\alpha \rightarrow \gamma$) transformation occurred and orientations from the ferrite γ -fibre, $\{111\}\langle uvw\rangle$, and the orientations lying within its spread, i.e. $\{332\}\langle uvw\rangle$, are in *K-S* relation with orientations from the α -fibre, $\{110\}\langle uvw\rangle$, of austenite. Brass type $\{110\}\langle 112\rangle$ orientation, which appeared within the austenite annealing texture (variant *A*), is in *K-S* relation with the $\{332\}\langle 113\rangle$ component of ferrite rolling texture. In the same way the $\{110\}\langle 001\rangle$ Goss orientation from austenite annealing texture (variant *B*) is related to the $\{111\}\langle 110\rangle$ and $\{332\}\langle 110\rangle$ orientations detected in ferrite after 85% of rolling reduction.

From X-ray phase analysis and texture measurements it results that contribution of deformation induced ($\gamma \rightarrow \alpha$) transformation depends on the applied variant of rolling, i.e. low or high reductions per pass, which resulted in different stress and strain distributions on the cross section of the rolled sheets [11]. In general strong ferrite textures were observed after 85% of deformation in comparison to one-phase steels for both rolling variants. However stronger deformation texture of ferrite was found within the centre layers of the sheets rolled with heavy drafts (variant *B*). In both cases formation of the rolling textures within the α -phase was a complex process which proceeded by deformation of ferrite, the occurrence of the ($\gamma \rightarrow \alpha$) phase transformation and subsequent deformation of the product α -phase (i.e. martensite).

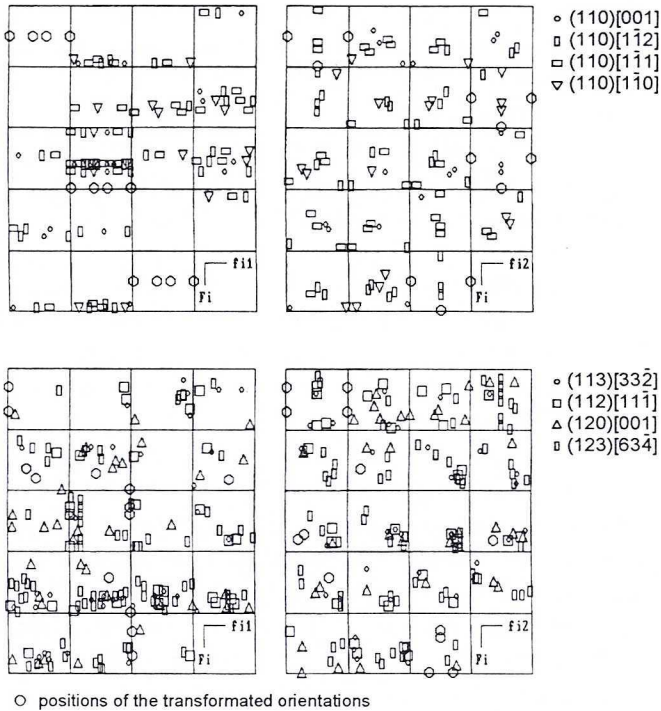


Fig. 7. Ideal orientations from the α -fibre (fcc), orientations from τ - and η -fibres, and S-type orientations transformed according to K-S relation (sections $\varphi_1 = \text{const}$ and $\varphi_2 = \text{const}$)

The austenite texture in the case of rolling variant *B* was a typical deformation texture for low SFE alloys, however weaker in comparison to the ferrite texture. Whereas in sheets rolled in variant *A*, the texture of austenite was nearly random. It seems, that deformation induced transformation of the austenite into the α -phase (i.e. martensite), within the centre layers of the sheets, was more pronounced in the case of variant *A*, i.e. small reductions in each roll pass [12].

After annealing the texture of austenite in the case of rolling variant *A* represents a typical deformation texture and similar result was obtained after transformation of ferrite deformation texture according to K-S relation (Fig. 3). The main components of the austenite texture, formed during annealing, are in K-S relation to the ferrite texture as the result of the inverse ($\alpha \rightarrow \gamma$) phase transformation. It should be noted however, that mutual orientation relationships between the austenite and the α -phase are satisfied not only by the main components but also orientations laying within their spread [9]. Therefore, in addition to ideal orientations (Fig. 7) also the experimental ODF's (Figs 3 and 4) were transformed according to K-S relation. Texture simulations indicate, that a smaller number of variants is engaged in texture transformation than predicted by K-S relation

and some kind of variant selection is assumed to take place [7, 10]. The appearance of some orientations within the austenite annealing texture allows to assume, that at the very beginning the α -phase, formed due to the deformation induced ($\gamma \rightarrow \alpha$) transformation, is changed back into austenite. It is thus concluded that during deformation austenite was constantly transformed into the α -martensite and as the result of annealing the austenite inherits its own rolling texture due to the inverse ($\alpha \rightarrow \gamma$) transformation. In general the austenite attains the texture typical for deformation textures of low SFE alloys and after annealing at 850°C for 1 and 10 hours the texture remains unchanged. Taking additionally into account the character of Debye's rings on back reflection patterns it was concluded that during annealing the "in situ" recrystallization was taking place. Thus the texture formation within both phases was the result of inverse ($\alpha \rightarrow \gamma$) transformation, recovery of the α -phase and "in situ" recrystallization of austenite.

5. Conclusions

1. Within the initial material after 85% of deformation the α -phase (ferrite) was dominating for both rolling variants, with the strong deformation texture having the fibrous character. The following orientation fibres were found within the rolling texture of the α -phase: α_1 -fibre $\rightarrow \langle 110 \rangle \parallel \text{RD}$; γ -fibre $\rightarrow \langle 111 \rangle \parallel \text{ND}$; ε -fibre $\rightarrow \langle 001 \rangle \parallel \text{ND}$.

2. Deformation texture of the γ -phase (austenite) was relatively weak or nearly random, depending on the applied rolling variant, due to the strain induced ($\gamma \rightarrow \alpha$) transformation resulting in a considerable change of the phase composition after deformation.

3. During annealing the ($\alpha \rightarrow \gamma$) phase transformation was taking place and the volume fraction of austenite increased at the expense of ferrite with increasing annealing time. At the very beginning the α -phase, formed due to the strain induced ($\gamma \rightarrow \alpha$) transformation, was changing back into austenite. Hence the austenite annealing texture may be essentially described by orientation fibres typical for deformation textures i.e.: α -fibre $\rightarrow \langle 110 \rangle \parallel \text{ND}$; τ -fibre $\rightarrow \langle 110 \rangle \parallel \text{TD}$; η -fibre $\rightarrow \langle 001 \rangle \parallel \text{RD}$.

4. With the applied rolling and annealing conditions the annealing texture of the α -phase was relatively weak, due to the transformation of ferrite into austenite and precipitation of the σ phase (FeCr), however the ferrite texture was typical for bcc metals.

5. In major part the orientation relations between both phases after rolling and annealing are well described by Kurdjumov-Sachs orientation relationship. However transformations of the major texture components as well as texture simulation, performed by transformation of experimental ODF's, indicate that not all of the 24 possible orientations are equally probable and some kind of variant selection was taking place.

Acknowledgements

The authors gratefully acknowledge financial support from the Polish Committee of Scientific Research (KBN) under the contract No 11. 110. 230.

REFERENCES

- [1] J. R. Davies ed., *Stainless Steels*, ASM Specialty Handbook; (1994).
- [2] C. H. Shek, G. J. Shen, J. K. L. Lai, B. J. Duggan, *Materials Science Forum*, **157—162**, 853 (1994).
- [3] N. Akdut, J. Foct, *Scripta Metall. et Mater.* **32**, 103, 109 (1995).
- [4] A. Maciosowski, S. Gorczyca, J. Pospiech, J. Jura, *Archives of Metall.* **23**, 217 (1978).
- [5] W. B. Hutchinson, K. Ushioda, G. Runsjö, *Mater. Science and Techn.* **1**, 728 (1985).
- [6] J. Komenda R. Sandstrom, *Materials Characterization* **31**, 155 (1993).
- [7] J. J. Jonas, M. P. Butron-Guillen, C. S. Da Costa Viana, *Proc. 11-th Int. Conf. on Textures of Materials, China*, 575 (1996).
- [8] M. P. Butron-Guillen, C. S. Da Costa Viana, J. J. Jonas, *Proc. 11-th Int. Conf. on Textures of Materials, China*, 604—610 (1996).
- [9] R. K. Ray, J. J. Jonas, *Int. Materials Reviews* **35**, 1, 1 (1990).
- [10] J. Pospiech, G. Bruckner, *Proc. 11-th Int. Conf. on Textures of Materials, China* 598 (1996).
- [11] W. Ratuszek, J. Ryś, K. Chruściel, *Archives of Metallurgy* **44**, 305 (1999).
- [12] J. Ryś, W. Ratuszek, J. Woźniak, K. Chruściel, *Inżynieria materiałowa* **20**, 601 (1999).
- [13] C. Donadille, R. Valle, P. Dervin, R. Penelle, *Acta Metall.* **37**, 1547 (1989).
- [14] H. Inagaki, *ISIJ International* **34**, 313 (1994).
- [15] K. Lucke, M. Holscher, *Textures and Microstructures* **14—18**, 585 (1991).
- [16] H. J. Bunge, *Mathematische Methoden der Texturanalyse*, Akademie-Verlag, Berlin (1969).

REVIEWED BY: PROF. DR HAB. INŻ. JAN POSPIECH

Received: 10 September 1999.